BIOCHEMISTRY
including biophysical chemistry & molecular biology

Article

pubs.acs.org/biochemistry

Active Site Structure and Peroxidase Activity of Oxidatively Modified Cytochrome *c* Species in Complexes with Cardiolipin

Daiana A. Capdevila,[†] Santiago Oviedo Rouco,[†] Florencia Tomasina,[‡] Verónica Tortora,[‡] Verónica Demicheli,[‡] Rafael Radi,[‡] and Daniel H. Murgida*[,†]

[†]Departamento de Química Inorgánica, Analítica y Química Física and INQUIMAE (CONICET-UBA), Facultad de Ciencias Exactas y Naturales, Universidad de Buenos Aires, Ciudad Universitaria, Pab. 2, piso 1, C1428EHA Buenos Aires, Argentina

[‡]Departamento de Bioquímica and Center for Free Radical and Biomedical Research, Facultad de Medicina, Universidad de la República, Montevideo, Uruguay

Supporting Information

ABSTRACT: We report a resonance Raman and UV−vis characterization of the active site structure of oxidatively modified forms of cytochrome *c* (Cyt-c) free in solution and in complexes with cardiolipin (CL). The studied post-translational modifications of Cyt-c include methionine sulfoxidation and tyrosine nitration, which lead to altered heme axial ligation and increased peroxidase activity with respect to those of the wild-type protein. In spite of the structural and activity differences between the protein variants free in solution, binding to CL liposomes induces in all cases the formation of a spectroscopically identical bis-His axial coordination conformer that more efficiently promotes lipid peroxidation. The spectroscopic results indicate that the bis-His form is in equilibrium with small amounts of high-spin species, thus suggesting a labile distal His ligand as the basis for the CL-induced increase in enzymatic activity observed for all protein variants. For Cyt-c nitrated at Tyr74 and sulfoxidized at Met80, the measured apparent binding affinities for CL are ∼4 times larger than for wild-type Cyt-c. On the basis of these results, we propose that these post-translational modifications may amplify the pro-apoptotic signal of Cyt-c under oxidative stress conditions at CL concentrations lower than for the unmodified protein.

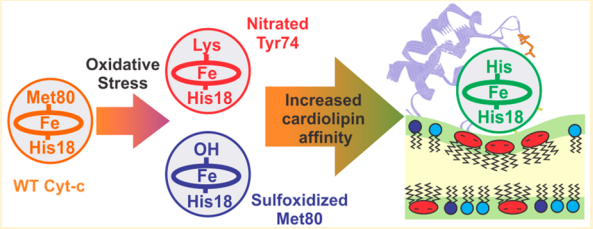

Cytochrome *c* (Cyt-c) is a 12.5 kDa soluble protein that contains a single heme prosthetic group covalently attached via two thioether bonds to cysteine residues in a CXXCH motif, where the histidine residue (His18) acts as the proximal axial ligand of the heme iron and Met80 is the sixth ligand on the distal side.[1,2]

In healthy mammalian cells, this protein is found trapped within the cristae and free in the intermembrane mitochondrial space, where it shuttles electrons between respiratory complexes III and IV embedded in the inner mitochondrial membrane (IMM).[1,3,4] Direct and phosphate-mediated electrostatic interactions of cationic Cyt-c with anionic and cationic lipid components of the IMM, respectively, as well as interactions with biomimetic self-assembled monolayers have proven to be crucial in defining critical thermodynamic, dynamic, and kinetic redox parameters of this electron carrier.[5−11] Among the different components of the IMM, cardiolipin (CL) is particularly relevant as it constitutes the only anionic phospholipid present and represents approximately 10−20% of the total lipid content of the IMM and a much smaller proportion for the outer mitochondrial membrane (OMM).[12,13] Different studies indicate that ∼15% of the available Cyt-c is actually bound to CL in healthy cells.[3,4] While the binding process is electrostatically driven, the resulting complex has been proposed to involve the insertion of one or two hydrocarbon chains of the lipid into hydrophobic channels of the protein.[14,15] Regardless of the mechanistic details, it is clear that the interactions of Cyt-c with CL and other anionic lipids induce changes in the protein tertiary and, to a lesser extent, secondary structure, as established by a variety of biophysical methods.[8,14,16−31] These structural changes include the breakage of the Fe−S(Met80) bond, thereby producing a significant increase in (lipo)peroxidase activity that has been implicated in the permeabilization of the mitochondrial membrane trough CL peroxidation.[32−37] Indeed, the early events of apoptosis include a significant increase in the CL levels in the OMM[32,36] and the concomitant increase in H_2O_2 concentration,[38] thus triggering Cyt-c-mediated lipid peroxidation, which is considered one of the pathways for prompting the liberation of pro-apoptotic factors to the cytosol.[33] Among them, the release of Cyt-c itself to form a multimeric complex with Apaf-1, ATP, and pro-caspase-9 (apoptosome) is one of the milestones in the cascade of events leading to cellular suicide.[39]

Thus, Cyt-c/CL interactions appear to be determinant both for sustaining and for terminating cellular life through regulation of disparate electron shuttling and peroxidatic functions of Cyt-c, respectively. In spite of this clear relevance,

Received: August 18, 2015
Revised: November 23, 2015
Published: December 1, 2015

DOI: 10.1021/acs.biochem.5b00922
Biochemistry 2015, 54, 7491−7504

the multiple spectroscopic studies reported for complexes of Cyt-c with CL and other model systems are sometimes contradictory, particularly regarding the axial coordination of the heme iron, which constitutes the active site for both protein functions. For example, resonance Raman (RR) determinations of Cyt-c bound to DOPG vesicles show the coexistence of variable proportions of the native axial coordination pattern (Met/His) with alternative hexa- and pentacoordinated species, such as bis-His, H_2O/His, and Fe−His, depending on the relative DOPG/Cyt-c concentrations.[24,25] Recent nuclear magnetic resonance studies of Cyt-c/SDS complexes confirm the bis-His form as the main component.[27] MCD studies of Cyt-c/CL complexes, on the other hand, suggest that the coordination pattern of the ferric protein at neutral pH is Lys/His and OH^-/His,[8] while RR studies of similar systems suggest the coexistence of Lys/His and pentacoordinated Fe-His species.[23] It has been proposed that the coordinated distal Lys in the so-called alkaline conformer may be more easily displaced than His to adopt a catalytically active five-coordinated form, thus favoring the Lys/His conformation.[16,40]

In general, it has been shown that the interactions of Cyt-c with lipids, but also mutations such as the naturally occurring G41S mutation, weaken the Met80−Fe bond and/or induce Ω loop perturbations that increase substrate accessibility to the active site, thus inducing the increase in peroxidase activity.[32,41,42]

The notion that different post-translational modifications of Cyt-c may act as inducers of the peroxidase activity adds additional complexity and raises new questions, particularly considering that the few available structural and functional studies mostly refer to the modified proteins free in solution and not to the relevant complexes with CL. Among these modifications, ortho-nitration of tyrosine residues has been reported for a variety of proteins under basal physiological conditions but is significantly augmented under diverse pathological conditions.[43] While mammalian Cyt-c contains four highly conserved Tyr residues at sequence positions 48, 67, 74, and 97, treatment with peroxynitrite leads to preferential mononitration of the solvent-exposed Tyr74 and Tyr97.[44] Nitration of Tyr97 appears to have no significant structural and/or functional consequences in terms of electron transport parameters and peroxidase activity. In contrast, the variant nitrated at Tyr74 (NO_2-Cyt_{74}) exhibits distinct features,[45,46] such as tyrosine deprotonation at neutral pH, which is coupled to an early alkaline transition characterized by Met → Lys exchange of the heme distal ligand. The structural change results in a loss of electron shuttling capability and an increase in peroxidatic activity of NO_2-Cyt_{74} at physiological pH.[46] Treatment of Cyt-c with reactive halogen species such as HOCl has also been reported to induce increased peroxidase activity, in this case ascribed to the HOCl-mediated oxidation of Met80.[47]

More recently, we have reported that Cyt-c interacts electrostatically with the most abundant lipid components of the mitochondrial membranes, phosphatidylcholine and phosphatidylethanolamine, through specific mediation of phosphate anions.[48] Under these conditions, the protein reacts efficiently with H_2O_2 at the submillimolar levels characteristic of the early pro-apoptotic stages.[38] The reaction results in the specific oxidation of the Met80 sulfur atom, thus yielding a stable peroxidase with a OH^-/His axial coordination pattern (SO-Cyt).[48]

In this work, we report a RR and UV−vis spectroscopic study of the conformational changes experienced at the level of the heme ligation pattern by oxidatively modified Cyt-c species upon interaction with unilamellar and multilamellar CL liposomes, and the concomitant changes in peroxidatic activity. The investigated biologically relevant post-translational modifications are tyrosine nitration and methionine oxidation, including NO_2-Cyt_{74}, NO_2-Cyt_{97}, and SO-Cyt. As a prerequisite for a meaningful comparison, we also revisit the axial coordination of wild-type Cyt-c in complexes with CL employing different pH conditions and the double mutant H33N/H26N to obtain a reliable spectral assignment.

EXPERIMENTAL PROCEDURES

Chemicals. Horse heart cytochrome *c* (Cyt-c) was purchased from Sigma-Aldrich (BioUltra, ≥99%). 1,2-Di[9-(*Z*)-octadecenoyl]-*sn*-glycero-3-phosphocholine (PC), tetraoleoyl cardiolipin (CL), and cardiolipin sodium salt from bovine heart (CL_{BH}) were from Avanti Polar Lipids. Hydrogen peroxide was from Mallinckrodt Baker, Inc., and Amplex Red Ultra was from Invitrogen.

Preparation and Purification of the Protein Variants. The protocols for production, purification, and characterization of the Cyt-c mutant H33N/H26N[49,50] and the post-translationally modified proteins SO-Cyt,[48] NO_2-Cyt_{74}, and NO_2-Cyt_{97}[46] were as described previously.

Preparation and Characterization of Liposomes. Liposomes were prepared using two different protocols, described below as methods A and B. In both cases, the vesicle size, distribution, and stability of the preparations were determined by dynamic light scattering (DLS; SLS-90 Plus/BI-MAS instrument equipped with a He−Ne laser operating at 632.8 nm and 15 mW).

In method A, an ethanolic stock solution of CL (20 mM) was rapidly injected into a vast excess of proper buffer to obtain a final solution containing <4% ethanol. This protocol produces multilamellar vesicles with an average radius of 100 nm [40 nm standard deviation (SD)] and a polydispersity of <0.3 (Figure 1A).

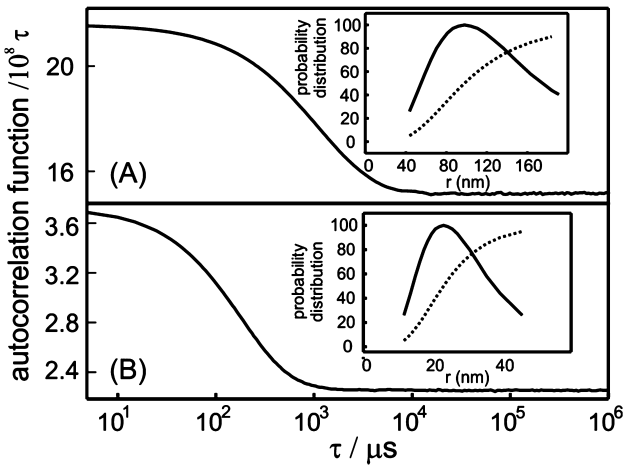

Figure 1. Typical DLS autocorrelation functions obtained for liposomes prepared by (A) method A and (B) method B as mentioned in the text. The data shown are the result of three acquisitions of 30 s. The insets show the size distributions (—) and the cumulative functions (···) obtained from the analysis of the autocorrelation functions.

DOI: 10.1021/acs.biochem.5b00922
Biochemistry 2015, 54, 7491−7504

In method B, unilamellar lipid vesicles were prepared by sonication of equimolar CL/PC mixtures. Appropriate amounts of lipid stock solutions were mixed in chloroform, evaporated to dryness under a gentle nitrogen stream, and then left under reduced pressure for 1.5 h to remove any residual solvent. The dry lipids were subsequently hydrated with 20 mM HEPES (pH 7) (with 100 μM DTPA) at room temperature to obtain lipid concentrations up to 5 mM. Such preparations were further sonicated five times for 30 s on ice using an ultrasonic probe tip sonicator. Identical results were obtained when sonication was conducted using an ultrasonic bath at 0 °C for 2 h. The liposomes were used immediately after preparation and presented an average radius of 25 nm (15 nm SD) and a polydispersity of <0.2 (Figure 1B).

For both types of liposomes, DLS characterizations performed in the absence and presence of Cyt-c and at the beginning and end of the spectroscopic experiments exhibit no differences within experimental error, thus indicating that both preparations are stable under these conditions throughout the experimental time window. All experiments were performed using the nonperoxidizable tetraoleoyl cardiolipin (CL), except for the determinations of O_2 consumption that were performed employing peroxidizable cardiolipin from bovine heart (CL_{BH}).

Spectroscopic Methods. Resonance Raman (RR) spectra were acquired employing a confocal microscope coupled to a single-stage spectrograph (Dilor XY; f = 800 mm) equipped with a 1800 lines/mm grating and a liquid nitrogen-cooled back-illuminated CCD detector (2048 × 512 pixels). The 413 nm line of a continuous wave krypton ion laser (~3 mW; Spectra Physics BeamLok 2060) or the 458 nm line of an argon ion laser (~8 mW; Coherent Innova 70c) was focused on the surface of a cylindrical quartz cuvette (Hellma) placed in a homemade rotating device by means of a long working distance objective (20×, NA 0.35), and the elastic scattering was rejected with Notch filters. The sample volumes were typically 200 μL, and the spectral accumulation times were between 10 and 120 s. Before each experiment, the spectrometer was calibrated employing Hg and Ne calibration lamps (Newport), and all the spectra were obtained simultaneously with the 435.833 nm line from the Hg calibration lamp as an internal spectroscopic standard to ensure reproducibility. The spectrometer parameters were set to obtain a 0.4 cm^{-1} increment per data point and a 3 cm^{-1} instrumental bandpass.

After background subtraction, the RR spectra were subjected to a component analysis as originally described by Döpner et al.[51] In this method, the experimental spectra are fitted using complete spectra of the different species involved, which are determined independently. The only adjustable parameters are the relative contributions of the different component spectra, while the spectral parameters of each component (positions, widths, and relative intensities of the different bands) are kept constant.

UV−visible absorption spectra were recorded either on a Thermo Scientific Evolution Array or on a Shimadzu UV-3600 spectrophotometer using a 1.0 nm spectral bandwidth. For UV−vis and combined UV−vis/RR experiments, protein solutions were placed into 1 cm path length quartz cuvettes (Hellma) equipped with a microstirrer (Labortechnik AG). Fluorescence experiments were performed either with a PTI-Quanta Master 4 or with a Thermo Varioskan Flash Multimode Reader instrument equipped with temperature control.

Ultracentrifugation. The binding of the Cyt-c variants to the liposomes was estimated using an ultracentrifugation assay as described previously[29] with minor modifications. Briefly, PC/CL dispersions (200 μM) were prepared in 20 mM buffer HEPES (pH 7.4, 1 mM EDTA) and brought into contact with Cyt-c at various concentrations (1−200 μM). Subsequently, the dispersion was equilibrated overnight at 4 °C. The lipid−protein complexes were separated from the free protein by ultracentrifugation for 80 min at 4 °C (160000g; Thermo scientific, Sorvall MX120+ microultracentrifuge). The free protein concentration was determined spectrophotometrically using a molar absorption coefficient of 106.1 mM^{-1} cm^{-1} at 410 nm.

Determination of Peroxidatic Activity. The assays were performed by adding 50 μM Amplex Red Ultra reagent and 25 μM H_2O_2 to a 0.5 μM protein solution in buffer HEPES [100 mM with 100 mM DTPA (pH 7.0)]. The fluorescence of the oxidation product, resorufin, was monitored at a λ_{em} of 585 nm (λ_{exc} = 570 nm) as a function of time using either a FLUOstar Optima plate fluorimeter (BMG Labtech) or a Varioskan Flash Multimode Reader (Thermo). The reaction rates were determined by a linear fit of the fluorescence intensity profile.

Measurement of Lipid Peroxidation. The lipoperoxidation activity was estimated by monitoring the oxygen consumption of samples placed in a 2.2 mL refrigerated chamber using a Clark-type electrode (Oxygraph 2k, Oroboros Instruments, Innsbruck, Austria). The protocol was as described previously[52] with only minor modifications. Briefly, CL_{BH}/PC liposomes (200 μM) were preincubated at 37 °C in 10 mM potassium phosphate buffer (pH 7.4, 100 μM DTPA) in the absence or presence of 20 μM WT Cyt-c, NO_2-Cyt_{74}, or SO-Cyt. Hydrogen peroxide (100 μM) was added to the liposome suspension after 15 min.

RESULTS AND DISCUSSION

Interactions of WT Cyt-c with CL Revisited. It has been extensively shown in previous work that the interactions of cationic Cyt-c with anionic model membranes usually lead to the breakage of the weak Met80−Fe bond, particularly for the ferric protein. The axial coordination of the heme iron in the complexes appears to be dependent on the model membrane and the specific conditions, and its assignment is not free of discrepancies.[8,23−25,27] Here we aim to correlate the active site structure and the peroxidatic activity of oxidatively modified Cyt-c species upon interactions with the anionic mitochondrial lipid CL. Therefore, as a prerequisite for a consistent evaluation of the effects of post-translational oxidative modifications, we first investigated the interactions of WT ferric Cyt-c with CL liposomes employing RR and UV−vis absorption as sensitive spectroscopic probes of the heme electronic structure. For comparative purposes, we selected two different liposome preparations that were recently employed for investigating Cyt-c/CL interactions.[8,37] Method A yields multilamellar single-component CL liposomes, while method B produces unilamellar 1:1 CL/PC vesicles (see Experimental Procedures for further details).

The injection of increasing amounts of an ethanolic solution of CL to WT Cyt-c (method A) results in the gradual loss of the CT absorption band at 695 nm and small blue-shifts of the remaining bands (Figure 2 and Figure S1). The underlying conformational transition appears to be quantitative at CL:Cyt-c molar ratios of ~25:1, as further injection of CL produces no additional spectral changes. Whereas the disappearance of the 695 nm band indicates the breakage of the Fe−Met80 bond,[53] the 3 nm downshift of the Soret and Q bands is consistent with

DOI: 10.1021/acs.biochem.5b00922
Biochemistry 2015, 54, 7491−7504

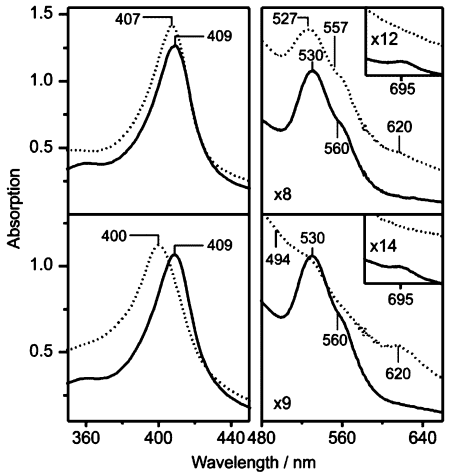

Figure 2. Electronic absorption spectra of ferric WT Cyt-c (top panels) and the H33N/H26N mutant (bottom panels). The solid and dotted lines correspond to 10 μM protein solutions in 20 mM HEPES (pH 7.0) before and after the addition of CL in 30:1 CL:protein molar ratio (method A), respectively.

the formation of a predominant non-native six-coordinated low-spin species (6cLS) that preserves the native proximal ligand His18.[24,25] Indeed, the absorption maxima closely resemble a misfolded Cyt-c fragment for which a bis-His axial coordination has been assigned.[28] In addition to these main spectral features, there is a hint of a very weak band at ~620 nm for relatively high CL concentrations, thus suggesting the presence of minor amounts of high-spin (HS) species in equilibrium with the main 6cLS alternative conformation.

Control experiments with the Cyt-c H33N/H26N double mutant, which retains the native axial coordination (Figure S2),[50] show more distinct spectral changes upon CL injection, including a larger downshift of the Soret band and relatively strong absorptions at 495 and 620 nm, thereby indicating a large population of HS species (Figure 2).

As shown in Figure 3, high-frequency RR bands ν_2–ν_4 and ν_{10} of WT Cyt-c experience upshifts of approximately 2–5 cm^{-1} upon addition of CL at lipid:protein molar ratios of ~25:1. These skeletal modes are sensitive to the porphyrin core size and electron density and constitute characteristic markers of the oxidation and spin states. Upshifts of this magnitude are indicative of the formation of alternative 6cLS species as a result of the replacement of Met80 with another strong-field distal ligand such as His, Lys, or OH^-.[9,24,25,54,55] Therefore, reference spectra for the Lys/His and OH^-/His 6cLS conformers were obtained from alkaline solutions of WT Cyt-c at pH 10.5 and 12.4, respectively.[55,56] As summarized in Figure 3 and Table 1, the high-frequency RR bands of the alkaline conformations exhibit relatively small but distinct differences with respect to the Cyt-c/CL complex, thus suggesting a different axial coordination. In good agreement with this conclusion, the Met/His, Lys/His, and OH^-/His forms of WT Cyt-c present low-frequency RR spectra with a qualitatively similar overall appearance and some quantitative differences, while the spectrum of the CL/Cyt-c complex is markedly different from those of all the other species. The differences include a significant intensity drop of the out-of-plane deformation modes γ_5 (731 cm^{-1}), γ_{12} (523 cm^{-1}), γ_{21} (569 cm^{-1}), and γ_{22} (446 cm^{-1}), thus suggesting an increased planarity of the heme that is compatible with a more symmetric axial coordination.[28,57] Moreover, the rise of a new band at 403 cm^{-1} strongly argues in favor of a bis-His coordination as this is the spectral position expected for the asymmetric stretching $\nu_{as}(Fe-Im_2)$ of nonequivalent histidine ligands.[28,58,59] Indeed, the spectrum of the Cyt-c/CL complex is very similar to that reported for the bis-His-coordinated N-fragment of Cyt-c[28] and also resembles very closely those of cytochrome *c* from *Methylophilus methylotrophus*[58] and of bis-His Cyt-c/SDS complexes.[24,25]

Control RR spectra of the double mutant H33N/H26N are also shown in Figure 3. While the spectra of WT Cyt-c and H33N/H26N recorded in the absence of CL are identical, the corresponding CL complexes exhibit sharp differences over the entire spectral range. The ν_3 envelope of the H33N/H26N/CL complex includes a band at 1504 cm^{-1}, i.e., compatible with a 6cLS species, and one additional band at ~1492 cm^{-1} (Figure S3) indicative of a HS form. The first one is compatible with either Lys/His[9,24,25,28,54,55] or N-terminal/His coordination, as shown for a misfolded comparable double mutant from yeast.[60] The position of the lower-frequency band is consistent with a Fe–His18 pentacoordinated heme (5cHS) according to previous assignments.[9,24,25,28,54,55]

On the basis of this evidence, we conclude that the heme iron in the neutral Cyt-c/CL complex presents a bis-His axial coordination with either His33 or His26 (or a mixture of both) as the distal ligand and His18 in the proximal position. Formation of similar bis-His species has been observed previously employing GuHCl and SDS reagents under both denaturating and nondenaturing conditions, and it was found that it may occur with a minimal loss of secondary structure, as indicated by IR and CD spectroscopy.[24,27] This process, however, necessarily implies tertiary structure changes associated with the translation of the histidine residues from the proximal to the distal side of the heme. Indeed, titration of Cyt-c with CL results in a substantial increase in the fluorescence emission of Trp59, which in the native Cyt-c conformation is quenched through Förster energy transfer with the heme (Figure S4). The emission maximum is found at ~330 nm, i.e., very similar to those of Cyt-c complexes with SDS, DOPS, and L-PG micelles, but blue-shifted with respect to those of urea- and GuHCl-denaturated Cyt-c, thereby indicating a more hydrophobic environment for Trp59 in the Cyt-c/CL complex compared to the fully denatured protein.[61–64] The increase in fluorescence shows a clear correlation with the population of bis-His species as determined by RR (Figure S4). In sharp contrast, alkalinization of Cyt-c solutions is not associated with a significant increase in Trp59 fluorescence, in line with the compact structure recently reported for the Lys/His alkaline conformer.[65]

Interestingly, RR spectroscopy shows that the addition of CL to the Lys/His alkaline isomer (pH 10.5) induces quantitative conversion to the same bis-His component obtained at neutral pH (Figure 3).

At CL:Cyt-c molar rations above 25:1, the ν_3 band of the neutral complex displays a low-intensity shoulder at ~1492 cm^{-1} (Figure S3) that suggests an equilibrium between the main bis-His component and a minor fraction of HS species, most likely 5cHS, in good agreement with the UV–vis data. For CL contents below these values, complete spectral data sets from Cyt-c titrations with CL can be quantitatively simulated employing only the fixed bis-His and Met/His RR spectral components in variable proportions (Figure S5), as described in Experimental Procedures. Similar results were obtained for

DOI: 10.1021/acs.biochem.5b00922
Biochemistry 2015, 54, 7491–7504

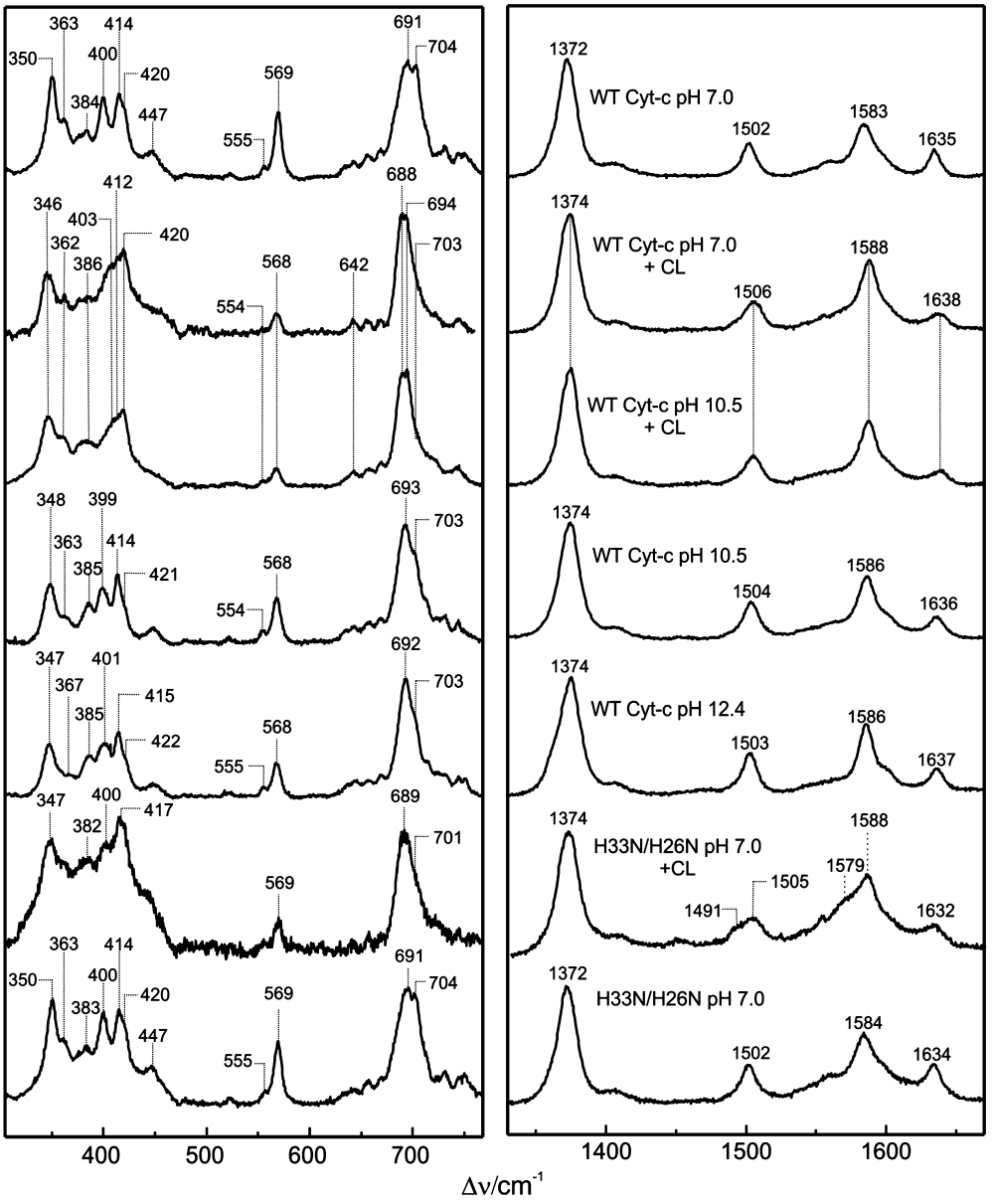

Figure 3. Low- and high-frequency RR spectra of 10 μM solutions of Cyt-c protein variants obtained with 413 nm excitation under different experimental conditions. From top to bottom the spectra correspond to WT Cyt-c at pH 7.0, WT Cyt-c at pH 7.0 with 250 μM CL, WT Cyt-c at pH 10.5 with 250 μM CL, WT Cyt-c at pH 10.5, WT Cyt-c at pH 12.4, H33N/H26N at pH 7.0 with 250 μM CL, and H33N/H26N at pH 7.0, respectively. The spectra are baseline-corrected and subtracted for ethanol contributions.

the NO_2-Cyt_{97} variant (see below). The relative intensity of each spectral component obtained in this analysis (I_i) is related to the relative concentration of the corresponding species (C_i) through a proportionality factor that reflects the reciprocal RR cross section: $C_i = I_i f_i / \sum_i I_i f_i$. The different proportionality factors were determined by comparing the intensities of the ν_4 bands of WT Cyt-c and NO_2-Cyt_{97} at pH 7.0, which represent pure Met/His species, with those obtained after addition of sufficient amounts of CL or base to achieve full conversion to the bis-His, Lys/His, and OH^-/His forms measured under, otherwise, identical conditions. Relative concentrations of the two alternative conformations of WT Cyt-c obtained in this way as a function of the added CL (method A) are shown in Figure 4A. Alternatively, the Met/His and bis-His relative concentrations were determined by deconvolution of the Soret absorption band into two Gaussian components with maxima at 406 and 409 nm (Figure S6 and Figure 4A), yielding results very similar to those of the RR quantification.

Titration of Cyt-c with unilamellar CL/PC liposomes (method B) produces qualitatively similar results. Indeed, both UV−vis and RR spectra can be quantitatively simulated employing the same Met/His and bis-His spectral components found for method A. The extent of the Met/His → bis-His conversion, however, is significantly lower in method B, thus underlying the importance of CL relative to the diluent PC component (Figure 4B), which is not expected to bind Cyt-c.

The data presented in Figure 4 can be rationalized in terms of coupled binding and conformational equilibria as shown in Scheme 1. The underlying simplifying assumptions are (i) the contribution of the HS form is negligibly small, (ii) after dissociation of the Cyt-c/CL complex the bis-His → Met/His back conversion is fast and complete, and (iii) $K_{bound}^{M \leftrightarrow H} \gg 1$.

DOI: 10.1021/acs.biochem.5b00922
Biochemistry 2015, 54, 7491−7504

Table 1. RR Spectral Parameters of the Different Axial Coordination Conformers of Ferric Cyt-c Determined under Soret Band Excitation (λ_{exc} = 413 nm)

	assigned axial coordination			
vibrational mode[a]	Met/His[b]	Lys/His[c]	OH^-/His[d]	bis-His[e]
	Low-Frequency Region			
ν_8	350	348	347	346
ν_{50}	363	363	367	362
$\delta(C_\beta C_c C_d)$	384	385	385	386
$\delta(C_\beta C_a S)$	400	–	–	–
$\nu_{as}(Fe-Im_2)$	–	–	–	403
$\delta(C_\beta C_a C_b)$	415, 421	414, 421	415, 422	412, 420
γ_{22}	446	448	449	–
γ_{12}	523	522	522	–
γ_{21}	555, 569	554, 568	555, 568	554, 568
ν_{48}	635, 642	634, 643	636, 644	642
γ_{20}	656, 669	658, 668	657, 669	658, 668
$\nu(C_aS)$	693	693	692	688, 694
ν_7	704	703	703	703
γ_{11}	725	725	725	721
γ_5	731	731	732	–
	High-Frequency Region			
ν_4	1372	1374	1374	1374
ν_3	1502	1504	1503	1506
ν_2	1583	1586	1586	1588
ν_{10}	1635	1636	1637	1638

[a]Assignment according to refs 28 and 56. [b]WT Cyt-c at pH 7.0. [c]WT Cyt-c at pH 10.5. [d]WT Cyt-c at pH 12.4. [e]WT Cyt-c at pH 7.0 in the presence of a 25-fold molar excess of CL.

On the basis of these considerations, the coupled equilibria depicted in Scheme 1 can be treated in terms of eq 1 with $K_{app} = K^{bind}_{Met/His} K^{M\leftrightarrow H}_{bound}$:

$$\log \frac{[\text{bis-His}]_{Tot}}{[\text{Met/His}]_{Tot}} = \log K_{app} + \log[CL] \quad (1)$$

This expression can be cast in a more general way by introducing an empirical parameter n to account for possible cooperativity effects:

$$\log \frac{[\text{bis-His}]_{Tot}}{[\text{Met/His}]_{Tot}} = \log(K_{app})^n + n \log[CL] \quad (2)$$

The results of this analysis, which are summarized in Figure 4, Table 2, and Table S1, yield $n \approx 1$ within experimental error, thus indicating the lack of significant phase separation or other possible cooperative effects under the experimental conditions presented here. The apparent binding constants are similar to values previously reported for Cyt-c and different anionic lipids.[25,26,34,66]

As mentioned above, mixed unilamellar liposomes yield incomplete Met/His → bis-His conversion even at a large excess of CL (Figure 4b), thus suggesting that either $K^{bind}_{Met/His}$ or $K^{M\leftrightarrow H}_{bound}$ is lower than that of the single-component multilamellar liposomes. In an attempt to distinguish between these two possibilities, we performed an independent assessment of the binding of Cyt-c to mixed liposomes employing a different experimental approach. For this control experiments, mixed liposomes [200 μM in CL; 20 mM HEPES (pH 7) and 1 mM EDTA] were incubated for 12 h with various final concentrations of Cyt-c. The lipid/protein complexes were then separated from the free protein by ultracentrifugation, and the concentration of Cyt-c in the supernatant was determined spectrophotometrically. The adsorption isotherm obtained in this way (Figure S7) is similar to those from previous reports.[29]

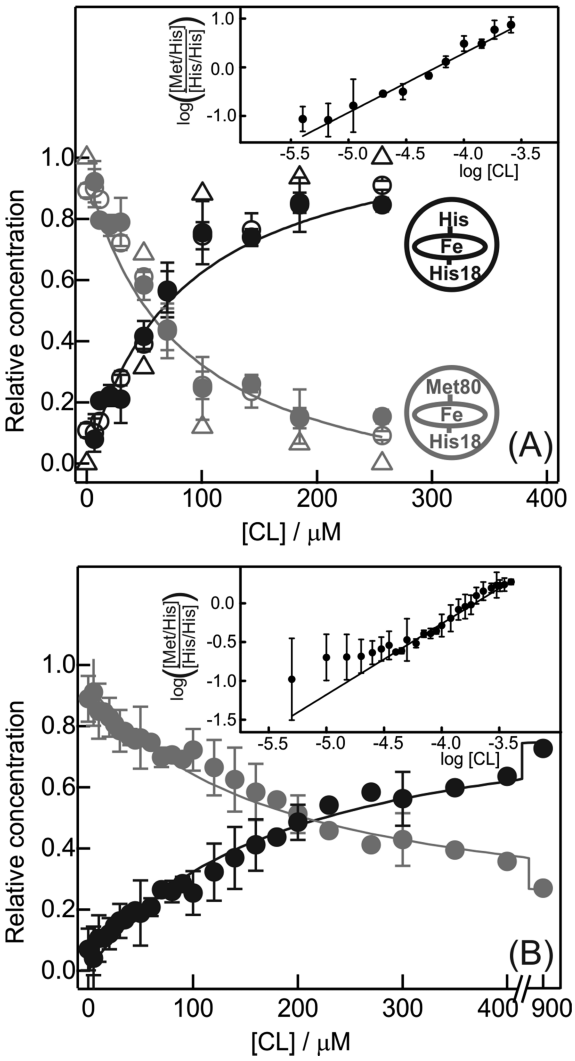

Figure 4. Relative concentrations of the Met/His (gray) and bis-His (black) species present in 10 μM solutions of WT Cyt-c [20 mM buffer HEPES (pH 7.0)] as a function of CL concentration. Panels A and B show data obtained with single-component multilamellar liposomes (method A) and mixed PC/CL unilamellar liposomes (method B), respectively. Data represented as solid symbols were obtained by component analysis of the high-frequency RR spectra (λ_{exc} = 413 nm). Empty circles and empty triangles correspond to data obtained from low-frequency RR and UV–vis spectra, respectively. The insets show the same data linearized and the corresponding fittings according to eq 2.

Scheme 1. Representation of the Coupled Binding and Conformational Equilibria of Cyt-c

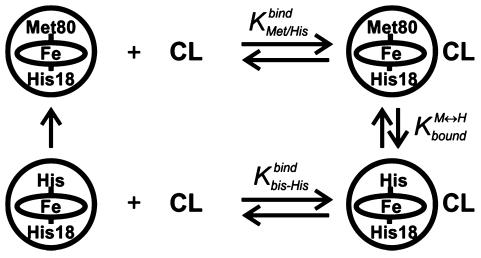

DOI: 10.1021/acs.biochem.5b00922
Biochemistry 2015, 54, 7491–7504

Table 2. Equilibrium Parameters Obtained by RR Spectroscopy for the Binding of the Different Cyt-c Variants to CL/PC Unilamellar Liposomes (method B)[a]

	Cyt-c	SO-Cyt	NO_2-Cyt_{74}	NO_2-Cyt_{97}
n	0.9 (0.2)	1.5 (0.3)	3.0 (0.8)	1.1 (0.2)
K_{app} ($\times 10^3$ M^{-1})	5.8 (0.3)	22 (1.0)	17 (1.0)	7.2 (0.3)
$K^{M\leftrightarrow H}_{bound}$	>12.5	–	–	>13
$K^{K\leftrightarrow H}_{bound}$	–	–	1.6	–
$K^{OH^-\leftrightarrow H}_{bound}$	–	4	–	–

[a]Results for multilamellar single-component liposomes are listed in Table S1. Standard deviations are indicated in parentheses. All the parameters were obtained using eqs 2–4 and correspond to the average of three independent experiments.

While the centrifugation assay reveals that for 10 μM total Cyt-c the concentration of lipid-bound protein is ~8 ± 3 μM, RR experiments yield $[\text{bis-His}]_{bound}$ = 4.9 ± 0.3 μM under similar conditions. Considering the large dispersion of the centrifugation data, this difference can be regarded as only a qualitative indication of a slightly lower value of $K^{M\leftrightarrow H}_{bound}$ in the mixed unilamellar liposomes. This conclusion is in agreement with the differences observed by RR for K_{app} and $K^{M\leftrightarrow H}_{bound}$ between the two different preparations (Table 2 and Table S1).

The differences observed between single-component and mixed liposomes are in line with previous observations showing that both the binding affinity and the structural changes of the bound protein and the membrane critically depend on the CL content in a very complex manner.[67]

CL-Induced Conformational Changes of Nitrated Cytochromes. In previous work, we have shown that the Cyt-c variant mononitrated at Tyr97 (NO_2-Cyt_{97}) is essentially indistinguishable from the unmodified WT protein in terms of redox properties, the pK_a for the alkaline transition, and structural features.[45,46] Indeed, the RR spectrum of NO_2-Cyt_{97} at neutral pH is undistinguishable from that of WT Cyt-c, displaying only the Met/His spectral component described in Table 1. Titration of NO_2-Cyt_{97} with multilamellar CL liposomes (method A) produces gradual conversion of the native Met/His conformation into the same bis-His component described above for WT Cyt-c/CL complexes (Figure S8). Quantitative treatment of these data in terms of Scheme 1 and eq 2 affords binding parameters similar to those of WT Cyt-c (Table 2 and Table S1). As for the WT protein, treatment of NO_2-Cyt_{97} with unilamellar mixed liposomes (method B) produces qualitatively similar results albeit with incomplete Met/His → bis-His conversion.

In contrast to NO_2-Cyt_{97}, the Cyt-c variant nitrated at Tyr74 (NO_2-Cyt_{74}) presents an "early" alkaline transition with a pK_a of 7.1,[45,46] such that at neutral pH the RR spectrum can be quantitatively simulated employing only two spectral components, the Met/His and Lys/His species described in Table 1 (Figure 5).[45,46]

Upon titration of NO_2-Cyt_{74} with multilamellar CL liposomes, we observe the gradual appearance of the bis-His component in the RR spectra at the expense of the Met/His and Lys/His species (Figure 5). In addition to the main Met/His, Lys/His, and bis-His species, we detect small amounts of a third component that presents spectral parameters typical of a HS heme (ν_2 = 1570, ν_3 = 1492, and ν_4 = 1369).[24] This species becomes more evident in complexes with unilamellar liposomes at CL:protein ratios of >10, but its contribution remains well below 10% for the entire range of CL concentrations studied (Figure S9).

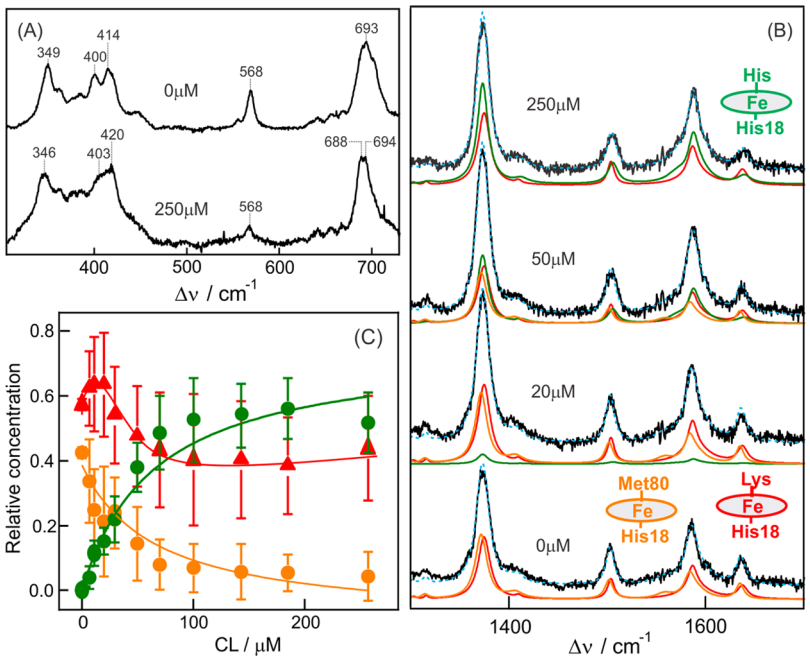

Figure 5. (A) Low-frequency RR spectra of 10 μM ferric NO_2-Cyt_{74} measured in the absence and presence of 250 μM CL (multilamellar liposomes). (B) High-frequency RR spectra of 10 μM ferric NO_2-Cyt_{74} as a function of CL concentration, as indicated at the top of each spectrum. Black lines are experimental spectra. Cyan lines are simulated spectra. Orange lines are Met/His spectral components. Red lines are Lys/His spectral components. Green lines are bis-His spectral components. The parameters of the different spectral components are summarized in Table 1. (C) Relative concentrations of the different species obtained from the spectra shown in panel B. All the spectra were measured with a λ_{exc} of 413 nm at pH 7.0 (20 mM HEPES). The spectra shown are baseline-corrected and subtracted for ethanol contributions.

DOI: 10.1021/acs.biochem.5b00922
Biochemistry 2015, 54, 7491–7504

Scheme 2. Representation of the Coupled Binding and Conformational Equilibria of NO_2-Cyt_{74}

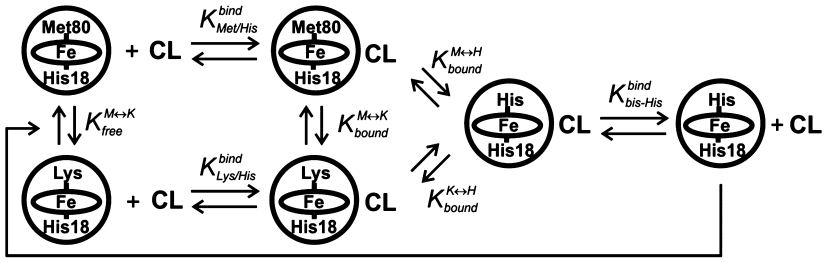

The coupled binding and conformational equilibria of NO_2-Cyt_{74} can be treated in terms of Scheme 2, where the minor HS species have been neglected for the sake of simplicity.

Here $[\text{bis-His}]_{free}$ and $[\text{Met/His}]_{bound}$ are neglected, as the bis-His species is not detected in the absence of CL and the Met/His component disappears after addition of excess CL. Moreover, given that the titrations were performed at pH ≈ pK_a, we can consider $[\text{Met/His}]_{free} \approx [\text{Lys/His}]_{free}$. Within these approximations, Scheme 2 affords an expression similar to eq 2 but with $K_{app} = K^{bind}_{Met/His} K^{M\leftrightarrow H}_{bound}$.

In addition, the conformational equilibrium of the bound Lys/His form can be expressed as

$$\log \frac{[\text{bis-His}]_{bound}}{[\text{Lys/His}]_{bound}} = \log \frac{[\text{bis-His}]_{Tot}}{[\text{Lys/His}]_{Tot} - [\text{Met/His}]_{Tot}} = \log K^{K\leftrightarrow H}_{bound} \quad (3)$$

As summarized in Table 2 and Table S1, K_{app}, and therefore $K^{M\leftrightarrow H}_{bound}$, is 2−3 times larger for NO_2-Cyt_{74} than for WT Cyt-c and NO_2-Cyt_{97}, thus indicating that nitration at position 74 confers a higher apparent affinity for CL and, probably, also a higher conformational susceptibility in the complex. The melting temperatures of the two nitrated variants, as determined from the temperature dependence of the Trp59 fluorescence, are very similar and only slightly lower than for WT Cyt-c (Table S2 and Figure S11), thereby suggesting that the differences cannot be ascribed to the intrinsic instability of NO_2-Cyt_{74}. The higher affinity is qualitatively confirmed by independent ultracentrifugation experiments shown in Figure S7. Moreover, the slightly but significantly higher n factor suggests that the NO_2-Cyt_{74} variant might be able to restructure the lipid membrane to a lager extent than previously observed for WT Cyt-c.[67]

To gain deeper insight into the interactions of NO_2-Cyt_{74} and NO_2-Cyt_{97} with CL, we performed titrations employing the 458 nm line from an argon laser for the RR monitoring. While the spectra recorded under Soret excitation display only vibrational modes from the heme, RR spectra obtained with 458 nm excitation show well-resolved bands of both the heme group and the nitrotyrosine residues with comparable intensities.[46] The detection is selective for the basic form of the nitrotyrosine trough the symmetric stretching of the nitro group (ν_{NO_2}) at ~1336 cm^{-1}, given that only this form but not the protonated species is in resonance with the 458 nm laser line.[46,68] As shown in Figure 6, the intensity of the ν_{NO_2} band decreases upon injection of CL, both for NO_2-Cyt_{74} and for NO_2-Cyt_{94}.

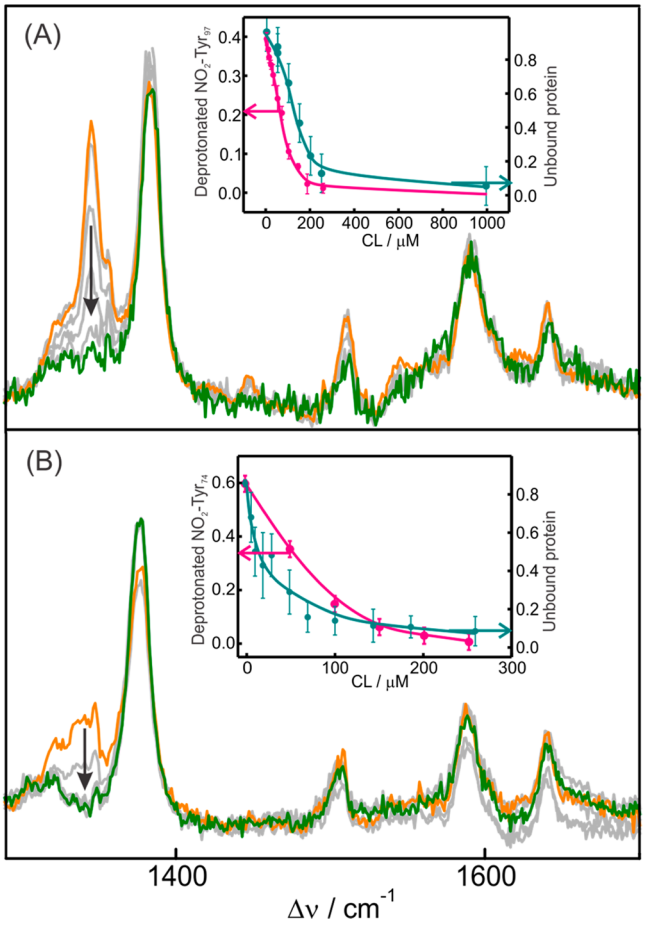

Figure 6. High-frequency RR spectra of 10 μM ferric samples of (A) NO_2-Cyt_{97} and (B) NO_2-Cyt_{74} measured with 458 nm excitation in the presence of different CL concentrations (method A; 20 mM HEPES at pH 7.0). The spectra are baseline-corrected and subtracted for ethanol contributions. Orange spectra were measured in the absence of CL. Green spectra are for a 25:1 molar ratio of CL to protein. The insets show the fractions of deprotonated nitrotyrosine (pink) and of unbound protein (cyan) determined by RR (λ_{exc} = 458 nm and λ_{exc} = 413 nm, respectively) as a function of CL concentration. Further details are given in the text.

This observation suggests that, upon binding to CL liposomes, the nitrated tyrosines sense a more hydrophobic environment that leads to protonation and concomitant loss of the resonance condition with the laser probe. For NO_2-Cyt_{74} free in solution, the population of deprotonated nitrotyrosine equals the fraction of protein in the Lys/His conformation.[46] Thus, the CL-induced intensity drop of the ν_{NO_2} band is likely to reflect structural changes at the distal site of the Lys/His conformer, particularly at the level of loop 71−85. Interestingly,

DOI: 10.1021/acs.biochem.5b00922
Biochemistry 2015, 54, 7491−7504

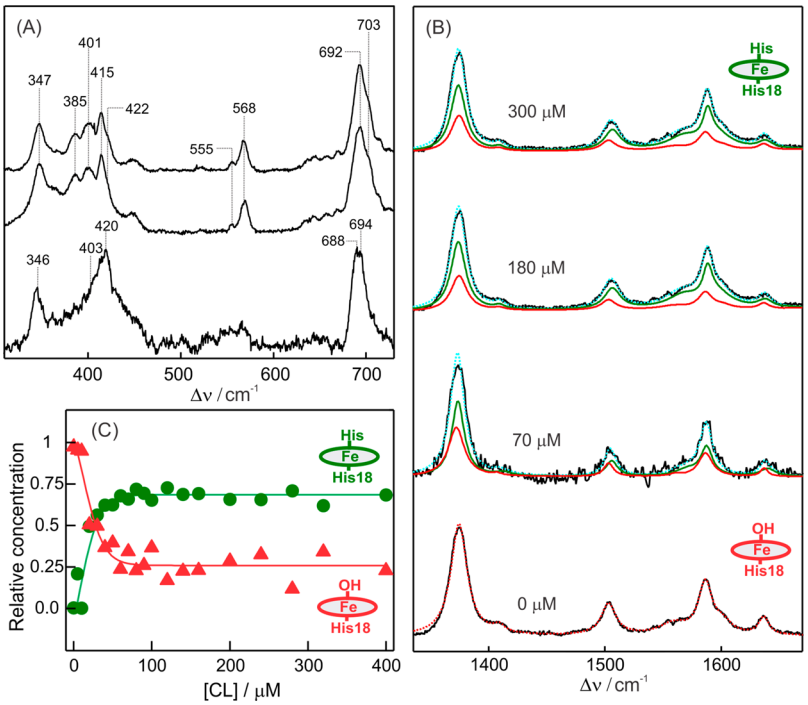

Figure 7. (A) Low-frequency RR spectra of 10 μM ferric WT Cyt-c at pH 12.4 (top), 10 μM ferric SO-Cyt at pH 7.0 (middle), and 10 μM ferric SO-Cyt at pH 7.0 in the presence of 300 μM multilamellar CL liposomes (bottom). (B) High-frequency RR spectra of 10 μM ferric SO-Cyt at pH 7.0 measured in the presence of increasing concentrations of CL (unilamellar PC/CL 1:1 liposomes), as indicated on top of each spectrum. Black solid lines are experimental spectra. Dotted cyan lines are simulated spectra. Red lines are OH^-/His spectral components. Green lines are His/His spectral components. (C) Relative concentrations of the spectral components obtained from panel A as a function of CL concentration. The symbols represent experimental data, and the lines are the best fit to eq 4. All the spectra shown were acquired with a λ_{exc} of 413 nm and are baseline-corrected and subtracted for ethanol contributions.

the apparent binding constant estimated from the data presented in Figure 6A is similar to the value obtained for WT Cyt-c from RR experiments under Soret excitation (Table S1).

Unlike NO_2-Cyt_{74}, the free NO_2-Cyt_{97} in solution presents only the native Met/His axial coordination and >80% of the nitrotyrosine residues deprotonated at neutral pH. In this case, the intensity drop of the ν_{NO_2} band cannot be correlated with changes at the level of loop 71−85 but, most likely, reflects the interactions of helix 85−105 with the liposomes, including partial unfolding at the C-terminus of this secondary structure element, in agreement with previous observations.[21,26,30,31] The apparent binding constant (K_{app}) obtained from the data in Figure 6B is 6 × 10^{-3} M^{-1}, which is lower than the value determined from RR experiments with 413 nm excitation under, otherwise, similar conditions (Table S1), thus indicating that only a fraction of the adsorbed species presents partial unfolding of helix 85−105, in agreement with previous proposals.[26]

CL-Induced Conformational Changes in Sulfoxidized Cytochrome. The controlled sulfoxidation of residue Met80 in a biomimetic environment has been recently shown to produce a stable species (SO-Cyt) with increased peroxidatic activity, thus suggesting a possible pro-apoptotic function for this post-translational modification of Cyt-c.[48] On the basis of its spectroscopic features and pH dependence of the reduction potential, the axial coordination of SO-Cyt at neutral pH has been assigned as HO^-/His.[48] To corroborate this coordination pattern, we compared the RR spectrum of neutral SO-Cyt with those obtained for WT Cyt-c at pH 10.5 and 12.4 as reference spectra of the Lys/His and OH^-/His forms, respectively. As summarized in Figure 7 and Table 1, the SO-Cyt variant exhibits close spectral similarities with the OH^-/His reference spectrum and small but reproducible differences with respect to the Lys/His form, thus further confirming the previous assignment. Upon addition of excess CL, the spectra display the characteristic changes that reveal the formation of the bis-His form in equilibrium with the OH^-/His species. Indeed, complete RR data sets corresponding to the titration of SO-Cyt with mixed CL liposomes (method B) can be quantitatively simulated employing variable amounts of the HO^-/His and bis-His spectral components described in Table 1 (Figure 7). As no other species are detected, the binding and conformational equilibria can be analyzed in terms of Scheme 1 but using HO^-/His and bis-His as the intervening species. As for the other protein variants, $[\text{bis-His}]_{free} = 0$, while the data in Figure 7C suggest that $[OH^-/\text{His}]_{free}$ is negligible at CL:SO-Cyt ratios of >10:1; therefore, $K_{bound}^{OH\leftrightarrow H} \approx 3$. With these approximations, and employing eq 4 with the equation $K_{app} = K_{OH/His}^{bind} K_{bound}^{OH\leftrightarrow H}$, we obtain the parameters reported in Table 2.

$$\log \frac{[\text{His/His}]_{Tot}}{[\text{OH/His}]_{Tot}} = \log(K_{app})^n + n \log[\text{CL}] \quad (4)$$

The apparent binding constant obtained in this way for SO-Cyt is ∼4 times larger than the value determined for the WT protein. Control experiments based on the temperature dependence of the Trp59 fluorescence yield a slightly lower melting temperature for SO-Cyt (Table S2 and Figure S11), thus suggesting an enhanced conformational flexibility of the modified protein as the basis of the higher apparent affinity.

DOI: 10.1021/acs.biochem.5b00922
Biochemistry 2015, 54, 7491−7504

Peroxidatic Activities of the CL/Protein Complexes. The peroxidase activities of the different Cyt-c variants were determined by employing the Amplex Red Ultra assay, by monitoring the fluorescence of the oxidation product resorufin as a function of time (see insets in Figure 8). In agreement with

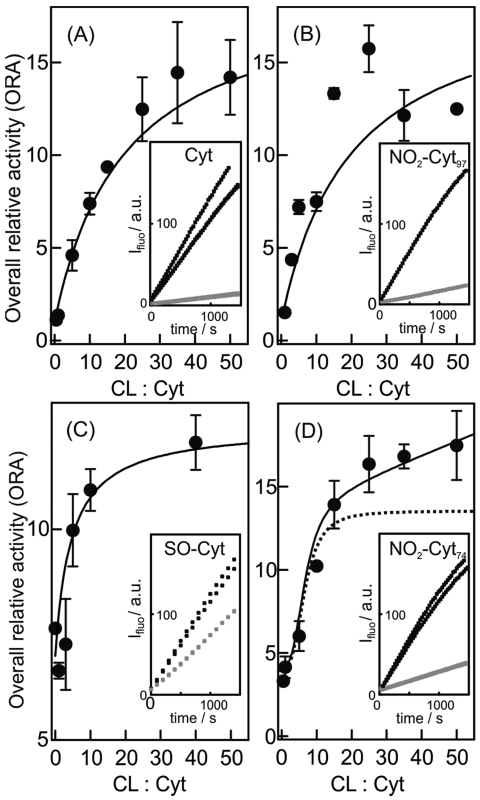

Figure 8. Overall relative peroxidatic activity determined by the Amplex Red assay for 1 μM solutions of (A) WT Cyt-c, (B) NO_2-Cyt_{97}, (C) SO-Cyt, and (D) NO_2-Cyt_{74} as a function of CL:Cyt molar ratio (method B). The solid lines represent the best fittings to eq 5, while the dotted line in panel D is the best fit to eq 5 plus an additional high-spin term, as indicated in the text. The insets show the emission of the resorufin product as a function of time for the different protein variants in the absence (gray) and presence (black) of a 50-fold molar excess of CL.

previous reports,[46,48] the catalytic activities obtained for the free proteins in neutral solutions decrease in the following order: SO-Cyt > NO_2-Cyt_{74} > NO_2-Cyt_{97} ≈ H33N/H26N ≈ WT Cyt-c (Table S2). Taking NO_2-Cyt_{74} at pH 8.5 and SO-Cyt at pH 7.0 as pure Lys/His and OH-/His species, respectively,[46,48] these assays show that the two alternative alkaline conformations present an enzymatic activity ~7-fold higher than that of the native Met/His form (Table 3). The enhanced peroxidase activity is in agreement with a recent report on a Cyt-c mutant that stabilizes a Lys/His conformer at nearly neutral pH.[65] These findings are somehow puzzling because the enzymatic activity requires dissociation of the distal ligand to allow H_2O_2 coordination, and therefore, one might expect the opposite trend on the basis of the higher stability of the Lys−Fe bond compared to that of the Met−Fe bond.[65,69] This apparent contradiction suggests that the structural details of the heme pocket and the changes associated with the opening of the heme crevice crucially define the thermodynamics and kinetics of the overall dissociation reaction. Indeed, molecular dynamics simulations show that, once the bond is broken, the energy cost for displacing the distal ligand apart from the iron is significantly higher for Met than for Lys.[46] A similar explanation may hold for the even higher peroxidase activity determined for the bis-His form in the peroxidase assays of complexes of Cyt-c with unilamellar CL liposomes (Figure 8A and Table 3).

Table 3. Peroxidase Activities of the Different Axial Coordination Conformers, Relative to the Native Met/His Species[a]

	Lys/His[b]	OH⁻/His[c]		bis-His[d]
protein variant	NO_2-Cyt_{74}	SO-Cyt	M80A	WT Cyt-c/CL
relative peroxidase activity	7.0 (1.0)	7.0 (1.0)	7.8 (0.8)	15.0 (1.0)

[a]Standard deviations are given in parentheses. [b]At pH 8.5 (from Figure 8B and ref 44). [c]From Figure 8C and ref 45. [d]From Figure 8A.

According to these estimates, the catalytic activity of the bis-His form is 15 times higher than for the Met/His conformer and twice the value obtained for Lys/His and OH^-/His. Note that values previously reported for the CL-induced increase in the peroxidase activity of WT Cyt-c span a broad range from 5 to 300.[32,36,70,71] This variability may arise from the different experimental conditions employed in terms of reducing substrate, buffer solution, and concentrations of CL and H_2O_2. The data summarized in Table 3 reflect intrinsic differences as all the determinations were consistently performed employing (i) low concentrations of H_2O_2 (12.5 μM) to prevent heme degradation, (ii) a moderate concentration of CL to ensure that all the protein is adsorbed and, at the same time, the liposomes remain unilamellar, (iii) a low-ionic strength HEPES buffer free of phosphate, (iv) addition of DTPA to prevent residual activity due to traces of free Fe^{3+}, and (v) the highly sensitive probe Amplex Red Ultra.

Addition of CL to all protein variants produces a gradual increase in the measured peroxidase activity (Figure 8). The SO-Cyt and NO_2-Cyt_{74} variants exhibit a steeper initial increase in activity compared to those of WT Cyt-c and NO_2-Cyt_{97}, but the values attained at high CL excess are relatively similar within experimental error (Figure 8 and Table S1). This finding is consistent with the fact that the bis-His conformer is the dominant species at high CL concentrations for all protein variants. Furthermore, it points out similarities at the level of the heme environment for the different protein/CL complexes that suggest a common interaction mechanism. Note, however, that control CL titrations monitored by the increase in Trp59 fluorescence show very similar behaviors for WT Cyt-c and NO_2-Cyt_{97}, but SO-Cyt and NO_2-Cyt_{74} exhibit significantly broader transitions, an ~10 nm red-shift of the emission maxima, and also higher intensity for NO_2-Cyt74 (Figure S12), thus pointing out the need for a detailed structural characterization of the protein/CL complexes at the atomistic level.

Interestingly, the activity versus CL concentration profiles shown in Figure 8 can be quantitatively simulated over the entire concentration range by simply considering the intrinsic activities of the different axial coordination conformers reported in Table 3 weighted by their relative concentrations as determined by RR. This relationship is expressed by eq 5, where ORA refers to the overall relative peroxidase activity:

$$\mathrm{ORA} = [\mathrm{Met/His}] + 7[\mathrm{Lys/His}] + 7[\mathrm{OH^-/His}] + 15[\mathrm{bis\text{-}His}] \quad (5)$$

DOI: 10.1021/acs.biochem.5b00922
Biochemistry 2015, 54, 7491−7504

Note that, while the symbols in Figure 8 represent the measured activities, the lines correspond to ORA simulations obtained with eq 5. For WT Cyt-c, NO_2-Cyt_{97}, and SO-Cyt, the theoretical curves reproduce reasonably well the experimental values, considering the experimental errors and the approximations involved. For the case of NO_2-Cyt_{74}, eq 5 is insufficient as it does not include the HS species detected spectroscopically (see the solid line in Figure 8D). Addition of a fifth term z[HS] to eq 5, where z is an adjustable parameter, produces a drastic improvement in the fitting (dotted line in Figure 8D) yielding z = 50 as the relative intrinsic activity for the HS form. This activity falls within the range reported for peroxidases,[40] which is remarkable considering the larger errors associated with the quantification of the minor HS species. The good correlations obtained in all cases confirm that, for the systems analyzed here, the intrinsic enzymatic activity is largely determined by the axial coordination pattern and can be transferred between protein variants. It is important to note that, according to the analysis of the coupled binding and conformational equilibria presented in the previous sections, the Met/His, Lys/His, and OH^-/His contributions in eq 5 are largely dominated by unbound protein, while the bis-His and HS contributions arise from CL-bound proteins. Thus, most likely, each conformer shares not only the axial coordination pattern but also some essential features of the heme environment that, altogether, determine the peroxidase activity. To further check this hypothesis, we determined the consumption of molecular oxygen for WT Cyt-c, NO_2-Cyt_{74}, and SO-Cyt in the presence of a 50-fold excess of mixed unilamellar liposomes, i.e., under conditions of maximal peroxidatic activity as determined in Figure 8. In contrast to the experiments described above, these determinations were performed employing a peroxidizable cardiolipin from bovine heart (CL_{BH}). The relative lipid peroxidation activities were estimated from the initial slope of O_2 consumption measured immediately after addition of H_2O_2.[52] As shown in Figure S10, NO_2-Cyt_{74} and SO-Cyt exhibit lipid peroxidation activities somewhat higher than that of the WT protein, but the differences are not pronounced and remain largely within experimental error.

Taken together, these findings show that the binding to CL of all the Cyt-c variants studied here induces a conformational transition to a lipoperoxidase competent species. The nitration of Tyr74 and the sulfoxidation of Met80, however, produce an increase in the apparent binding affinity for CL that correlates with a different exposure of Trp59 and results in a larger increase in peroxidase activity at lower CL concentrations. Thus, these post-translational modifications are likely to amplify the pro-apoptotic function of Cyt-c.

Recent studies have demonstrated that Cyt-c can be post-translationally phosphorylated at tyrosines 48 and 97 in a tissue specific manner.[72] Interestingly, a Cyt-c variant that includes a phosphomimetic substitution of Tyr48 presents an affinity for CL 30% lower than that of the WT protein and requires a high CL concentration to induce peroxidase activity,[72] in sharp contrast with Tyr74 nitration.

CONCLUSIONS

The binding of WT Cyt-c to CL-containing liposomes induces protein structural changes that result in the replacement of the distal ligand Met80 with a histidine residue, thus yielding a bis-His alternative conformation. RR experiments show that the bis-His form is in equilibrium with minor amounts of high-spin species, most likely pentacoordinated, thereby suggesting a certain lability of the distal His ligand. In agreement with this conclusion, the bis-His alternative conformation presents a peroxidase activity 15-fold higher than that of the Met/His native protein and twice the values determined for the Lys/His and OH^-/His alkaline conformations. Post-translational nitration of Tyr97 (NO_2-Cyt_{97}) has no significant effects on the structure, redox properties, peroxidatic activity, or apparent binding to CL liposomes. Nitration of Tyr74 (NO_2-Cyt_{74}), in sharp contrast, presents an early alkaline transition that results in the coexistence of similar populations of Met/His and Lys/His species at neutral pH, with the latter presenting a 7-fold increase in peroxidatic activity with respect to the native axial coordination. Similar to that of the WT protein, binding of NO_2-Cyt_{74} to CL liposomes results in the formation of bis-His species plus a minor fraction of a HS form at the expense of the Met/His and Lys/His populations. The displacement of the conformational equilibria of nitrated Cyt-c toward the bis-His conformation is qualitatively consistent with previous observations of electrostatic complexes between monotyrosine mutants and SAM-coated electrodes.[73] Interestingly, the sulfoxidized protein SO-Cyt, which presents OH^-/His axial coordination in neutral solution, also undergoes conversion to the bis-His form upon binding to CL, which results in a 2-fold increase in peroxidase activity. For all the protein variants studied here (WT Cyt-c, NO_2-Cyt_{97}, NO_2-Cyt_{74}, and SO-Cyt), titrations with CL liposomes yield clear correlations of the measured overall peroxidase activities with the intrinsic activities of the axial coordination conformers weighted by their relative concentrations. In the presence of a sufficient excess of CL, all protein variants are dominated by the bis-His alternative conformational state and present similar peroxidase and lipoperoxidase activities. Most likely, the essential features of the heme environment that, together with the axial coordination, determine the peroxidatic activity are also comparable to some extent. Therefore, although post-translational nitration and sulfoxidation are associated with significant and differential increases in peroxidatic activities in solution in the order SO-Cyt > NO_2-Cyt_{74} > NO_2-Cyt_{97} ≈ WT Cyt-c, these differences appear not to be relevant after binding to a large excess of CL. On the other hand, the apparent binding constants of SO-Cyt and NO_2-Cyt_{74} to CL/PC liposomes are nearly 4 times larger than for the unmodified Cyt-c, as determined by RR spectroscopy, which is consistent with a differential exposure of Trp59. The higher apparent affinity and thermal instability are paralleled by apparent binding cooperativity, which may be related to an enhanced ability to induce partial restructuring of the lipid bilayer. Further work to clarify these issues is currently ongoing.

These results suggest that nitration of Tyr74 and sulfoxidation of Met80 may result in amplification of the pro-apoptotic signal because of their higher affinities for CL that induce the formation of catalytically competent species for lipid peroxidation at CL concentrations lower than for the unmodified protein.

ASSOCIATED CONTENT

Supporting Information

The Supporting Information is available free of charge on the ACS Publications website at DOI: 10.1021/acs.biochem.5b00922.

DOI: 10.1021/acs.biochem.5b00922
Biochemistry 2015, 54, 7491−7504

RR and UV−vis titrations, binding isotherms, and lipid peroxidation experiments (PDF)

AUTHOR INFORMATION

Corresponding Author

*E-mail: dhmurgida@qi.fcen.uba.ar.

Funding

D.H.M. is funded by ANPCyT (Grants PICT 2010-070 and 2011-1249) and UBACyT (Grant 20020130100206BA). R.R. is funded by ANII (Grant FCE 104233) and Universidad de la República (CSIC Grupos and EI CEINBIO). Additional support was provided by CeBEM (Centro de Biología Estructural del Mercosur). D.A.C. and S.O.R. are recipients of CONICET and UBA fellowships, respectively. F.T. is partially supported by a fellowship from Universidad de la República. D.H.M. is staff member of CONICET.

Notes

The authors declare no competing financial interest.

ABBREVIATIONS

Cyt-c, cytochrome *c*; CL, tetraoleoyl cardiolipin; IMM, inner mitochondrial membrane; OMM, outer mitochondrial membrane; RR, resonance Raman; DOPG, 1,2-dioleoyl-*sn*-glycero-3-phospho-*rac*-(1-glycerol) sodium salt; SDS, sodium dodecyl sulfate; NO_2-Cyt_{74}, cytochrome *c* nitrated at Tyr74; NO_2-Cyt_{97}, cytochrome *c* nitrated at Tyr97; SO-Cyt, cytochrome *c* with sulfoxidized Met80; PC, 1,2-di[9(*Z*)-octadecenoyl]-*sn*-glycero-3-phosphocholine; CL_{BH}, cardiolipin sodium salt from bovine heart; CT, charge transfer; 6cLS, six-coordinated low-spin; HS, high-spin; WT, wild type; 5cHS, pentacoordinated high-spin; GuHCl, guanidine hydrochloride; DOPS, 1,2-dioleoyl-*sn*-glycero-3-phospho-L-serine sodium salt; L-PG, lysyl-phosphatidylglycerol.

REFERENCES

(1) *Cytochrome c: A multidisciplinary approach* (1995) University Science Books, Sausalito, CA.

(2) Bushnell, G. W., Louie, G. V., and Brayer, G. D. (1990) High-resolution three-dimensional structure of horse heart cytochrome c. *J. Mol. Biol. 214*, 585−595.

(3) Cortese, J. D., Voglino, A. L., and Hackenbrock, C. R. (1995) Persistence of cytochrome c binding to membranes at physiological mitochondrial intermembrane space ionic strength. *Biochim. Biophys. Acta, Bioenerg. 1228*, 216−228.

(4) Schug, Z. T., and Gottlieb, E. (2009) Cardiolipin acts as a mitochondrial signalling platform to launch apoptosis. *Biochim. Biophys. Acta, Biomembr. 1788*, 2022−2031.

(5) Salamon, Z., and Tollin, G. (1997) Interaction of horse heart cytochrome c with lipid bilayer membranes: Effects on redox potentials. *J. Bioenerg. Biomembr. 29*, 211−221.

(6) Alvarez-Paggi, D., Castro, M. A., Tortora, V., Castro, L., Radi, R., and Murgida, D. H. (2013) Electrostatically Driven Second-Sphere Ligand Switch between High and Low Reorganization Energy Forms of Native Cytochrome c. *J. Am. Chem. Soc. 135*, 4389−4397.

(7) Basova, L. V., Kurnikov, I. V., Wang, L., Ritov, V. B., Belikova, N. A., Vlasova, I. I., Pacheco, A. A., Winnica, D. E., Peterson, J., Bayir, H., Waldeck, D. H., and Kagan, V. E. (2007) Cardiolipin switch in mitochondria: Shutting off the reduction of cytochrome c and turning on the peroxidase activity. *Biochemistry 46*, 3423−3434.

(8) Bradley, J. M., Silkstone, G., Wilson, M. T., Cheesman, M. R., and Butt, J. N. (2011) Probing a Complex of Cytochrome c and Cardiolipin by Magnetic Circular Dichroism Spectroscopy: Implications for the Initial Events in Apoptosis. *J. Am. Chem. Soc. 133*, 19676−19679.

(9) Murgida, D. H., and Hildebrandt, P. (2004) Electron-transfer processes of cytochrome c at interfaces. New insights by surface-enhanced resonance Raman spectroscopy. *Acc. Chem. Res. 37*, 854−861.

(10) Alvarez-Paggi, D., Zitare, U., and Murgida, D. H. (2014) The role of protein dynamics and thermal fluctuations in regulating cytochrome c/cytochrome c oxidase electron transfer. *Biochim. Biophys. Acta, Bioenerg. 1837*, 1196−1207.

(11) Capdevila, D. A., Marmisollé, W. A., Williams, F. J., and Murgida, D. H. (2013) Phosphate mediated adsorption and electron transfer of cytochrome c. A time-resolved SERR spectroelectrochemical study. *Phys. Chem. Chem. Phys. 15*, 5386−5394.

(12) Garcia Fernandez, M., Troiano, L., Moretti, L., Nasi, M., Pinti, M., Salvioli, S., Dobrucki, J., and Cossarizza, A. (2002) Early changes in intramitochondrial cardiolipin distribution during apoptosis. *Cell Growth Diff. 13*, 449−455.

(13) Osman, C., Voelker, D. R., and Langer, T. (2011) Making heads or tails of phospholipids in mitochondria. *J. Cell Biol. 192*, 7−16.

(14) Sinibaldi, F., Howes, B. D., Piro, M. C., Polticelli, F., Bombelli, C., Ferri, T., Coletta, M., Smulevich, G., and Santucci, R. (2010) Extended cardiolipin anchorage to cytochrome c: a model for protein-mitochondrial membrane binding. *JBIC, J. Biol. Inorg. Chem. 15*, 689−700.

(15) Tuominen, E. K. J., Wallace, C. J. A., and Kinnunen, P. K. J. (2002) Phospholipid-cytochrome c interaction. Evidence for the extended lipid anchorage. *J. Biol. Chem. 277*, 8822−8826.

(16) Muenzner, J., and Pletneva, E. V. (2014) Structural transformations of cytochrome c upon interaction with cardiolipin. *Chem. Phys. Lipids 179*, 57−63.

(17) Ranieri, A., Bortolotti, C. A., Battistuzzi, G., Borsari, M., Paltrinieri, L., Di Rocco, G., and Sola, M. (2014) Effect of motional restriction on the unfolding properties of a cytochrome c featuring a His/Met-His/His ligation switch. *Metallomics 6*, 874−884.

(18) Kawai, C., Ferreira, J. C., Baptista, M. S., and Nantes, I. L. (2014) Not only oxidation of cardiolipin affects the affinity of cytochrome c for lipid bilayers. *J. Phys. Chem. B 118*, 11863−11872.

(19) Mugnol, K. C. U., Ando, R. A., Nagayasu, R. Y., Faljoni-Alario, A., Brochsztain, S., Santos, P. S., Nascimento, O. R., and Nantes, I. L. (2008) Spectroscopic, structural, and functional characterization of the alternative low-spin state of horse heart cytochrome c. *Biophys. J. 94*, 4066−4077.

(20) Zucchi, M. R., Nascimento, O. R., Faljoni-Alario, A., Prieto, T., and Nantes, I. L. (2003) Modulation of cytochrome c spin states by lipid acyl chains: A continuous-wave electron paramagnetic resonance (CW-EPR) study of haem iron. *Biochem. J. 370*, 671−678.

(21) Nantes, I. L., Zucchi, M. R., Nascimento, O. R., and Faljoni-Alario, A. (2001) Effect of heme iron valence state on the conformation of cytochrome c and its association with membrane interfaces: A CD and EPR investigation. *J. Biol. Chem. 276*, 153−158.

(22) Sinibaldi, F., Fiorucci, L., Patriarca, A., Lauceri, R., Ferri, T., Coletta, M., and Santucci, R. (2008) Insights into cytochrome c-cardiolipin interaction. Role played by ionic strength. *Biochemistry 47*, 6928−6935.

(23) Sinibaldi, F., Howes, B. D., Droghetti, E., Polticelli, F., Piro, M. C., Di Pierro, D., Fiorucci, L., Coletta, M., Smulevich, G., and Santucci, R. (2013) Role of Lysines in Cytochrome c-Cardiolipin Interaction. *Biochemistry 52*, 4578−4588.

(24) Oellerich, S., Wackerbarth, H., and Hildebrandt, P. (2002) Spectroscopic characterization of nonnative conformational states of cytochrome c. *J. Phys. Chem. B 106*, 6566−6580.

(25) Oellerich, S., Lecomte, S., Paternostre, M., Heimburg, T., and Hildebrandt, P. (2004) Peripheral and integral binding of cytochrome c to phospholipids vesicles. *J. Phys. Chem. B 108*, 3871−3878.

(26) Hanske, J., Toffey, J. R., Morenz, A. M., Bonilla, A. J., Schiavoni, K. H., and Pletneva, E. V. (2012) Conformational properties of cardiolipin-bound cytochrome c. *Proc. Natl. Acad. Sci. U. S. A. 109*, 125−130.

(27) Simon, M., Metzinger-Le Meuth, V., Chevance, S., Delalande, O., and Bondon, A. (2013) Versatility of non-native forms of human

DOI: 10.1021/acs.biochem.5b00922
Biochemistry 2015, 54, 7491−7504

cytochrome c: PH and micellar concentration dependence. *JBIC, J. Biol. Inorg. Chem. 18*, 27−38.
(28) Santoni, E., Scatragli, S., Sinibaldi, F., Fiorucci, L., Santucci, R., and Smulevich, G. (2004) A model for the misfolded bis-His intermediate of cytochrome c: The 1−56 N-fragment. *J. Inorg. Biochem. 98*, 1067−1077.
(29) Heimburg, T., Angerstein, B., and Marsh, D. (1999) Binding of peripheral proteins to mixed lipid membranes: Effect of lipid demixing upon binding. *Biophys. J. 76*, 2575−2586.
(30) Heimburg, T., and Marsh, D. (1993) Investigation of secondary and tertiary structural changes of cytochrome c in complexes with anionic lipids using amide hydrogen exchange measurements: An FTIR study. *Biophys. J. 65*, 2408−2417.
(31) Choi, S., and Swanson, J. M. (1995) Interaction of cytochrome c with cardiolipin: an infrared spectroscopic study. *Biophys. Chem. 54*, 271−278.
(32) Kagan, V. E., Bayır, H. A., Belikova, N. A., Kapralov, O., Tyurina, Y. Y., Tyurin, V. A., Jiang, J. F., Stoyanovsky, D. A., Wipf, P., Kochanek, P. M., Greenberger, J. S., Pitt, B., Shvedova, A. A., and Borisenko, G. (2009) Cytochrome c/cardiolipin relations in mitochondria: a kiss of death. *Free Radical Biol. Med. 46*, 1439−1453.
(33) Huttemann, M., Pecina, P., Rainbolt, M., Sanderson, T. H., Kagan, V. E., Samavati, L., Doan, J. W., and Lee, I. (2011) The multiple functions of cytochrome c and their regulation in life and death decisions of the mammalian cell: From respiration to apoptosis. *Mitochondrion 11*, 369−381.
(34) Kapralov, A. A., Kurnikov, I. V., Vlasova, I. I., Belikova, N. A., Tyurin, V. A., Basova, L. V., Zhao, Q., Tyurina, Y. Y., Jiang, J. F., Bayir, H., Vladimirov, Y. A., and Kagan, V. E. (2007) The hierarchy of structural transitions induced in cytochrome c by anionic phospholipids determines its peroxidase activation and selective peroxidation during apoptosis in cells. *Biochemistry 46*, 14232−14244.
(35) Tyurina, Y. Y., Kini, V., Tyurin, V. A., Vlasova, I. I., Jiang, J. F., Kapralov, A. A., Belikova, N. A., Yalowich, J. C., Kurnikov, I. V., and Kagan, V. E. (2006) Mechanisms of cardiolipin oxidation by cytochrome c: Relevance to pro- and antiapoptotic functions of etoposide. *Mol. Pharmacol. 70*, 706−717.
(36) Kagan, V. E., Tyurin, V. A., Jiang, J. F., Tyurina, Y. Y., Ritov, V. B., Amoscato, A. A., Osipov, A. N., Belikova, N. A., Kapralov, A. A., Kini, V., Vlasova, I. I., Zhao, Q., Zou, M. M., Di, P., Svistunenko, D. A., Kurnikov, I. V., and Borisenko, G. G. (2005) Cytochrome c acts as a cardiolipin oxygenase required for release of proapoptotic factors. *Nat. Chem. Biol. 1*, 223−232.
(37) Kapralov, A. A., Yanamala, N., Tyurina, Y. Y., Castro, L., Samhan-Arias, A., Vladimirov, Y. A., Maeda, A., Weitz, A. A., Peterson, J., Mylnikov, D., Demicheli, V., Tortora, V., Klein-Seetharaman, J., Radi, R., and Kagan, V. E. (2011) Topography of tyrosine residues and their involvement in peroxidation of polyunsaturated cardiolipin in cytochrome c/cardiolipin peroxidase complexes. *Biochim. Biophys. Acta, Biomembr. 1808*, 2147−2155.
(38) Giorgio, M., Trinei, M., Migliaccio, E., and Pelicci, P. G. (2007) Hydrogen peroxide: A metabolic by-product or a common mediator of ageing signals? *Nat. Rev. Mol. Cell Biol. 8*, 722−728.
(39) Kulikov, A. V., Shilov, E. S., Mufazalov, I. A., Gogvadze, V., Nedospasov, S. A., and Zhivotovsky, B. (2012) Cytochrome c: The Achilles' heel in apoptosis. *Cell. Mol. Life Sci. 69*, 1787−1797.
(40) Diederix, R. E. M., Ubbink, M., and Canters, G. W. (2002) Peroxidase activity as a tool for studying the folding of c-type cytochromes. *Biochemistry 41*, 13067−13077.
(41) Rajagopal, B. S., Edzuma, A. N., Hough, M. A., Blundell, K. L., Kagan, V. E., Kapralov, A. A., Fraser, L. A., Butt, J. N., Silkstone, G. G., Wilson, M. T., Svistunenko, D. A., and Worrall, J. A. (2013) The hydrogen-peroxide-induced radical behaviour in human cytochrome c-phospholipid complexes: implications for the enhanced pro-apoptotic activity of the G41S mutant. *Biochem. J. 456*, 441−452.
(42) Josephs, T. M., Morison, I. M., Day, C. L., Wilbanks, S. M., and Ledgerwood, E. C. (2014) Enhancing the peroxidase activity of cytochrome c by mutation of residue 41: Implications for the peroxidase mechanism and cytochrome c release. *Biochem. J. 458*, 259−265.
(43) Radi, R. (2013) Protein Tyrosine Nitration: Biochemical Mechanisms and Structural Basis of Functional Effects. *Acc. Chem. Res. 46*, 550−559.
(44) Souza, J. M., Castro, L., Cassina, A. M., Batthyany, C., and Radi, R. (2008) Nitrocytochrome c: Synthesis, purification, and functional studies. *Methods Enzymol. 441*, 197−215.
(45) Abriata, L. A., Cassina, A., Tortora, V., Marin, M., Souza, J. M., Castro, L., Vila, A. J., and Radi, R. (2009) Nitration of solvent-exposed tyrosine 74 on cytochrome c triggers heme iron-methionine 80 bond disruption. Nuclear magnetic resonance and optical spectroscopy studies. *J. Biol. Chem. 284*, 17−26.
(46) Capdevila, D. A., Álvarez-Paggi, D., Castro, M. A., Tórtora, V., Demicheli, V., Estrín, D. A., Radi, R., and Murgida, D. H. (2014) Coupling of tyrosine deprotonation and axial ligand exchange in nitrocytochrome c. *Chem. Commun. 50*, 2592−2594.
(47) Chen, Y. R., Deterding, L. J., Sturgeon, B. E., Tomer, K. B., and Mason, R. P. (2002) Protein oxidation of cytochrome C by reactive halogen species enhances its peroxidase activity. *J. Biol. Chem. 277*, 29781−29791.
(48) Capdevila, D. A., Marmisolle, W. A., Tomasina, F., Demicheli, V., Portela, M., Radi, R., and Murgida, D. H. (2015) Specific methionine oxidation of cytochrome c in complexes with zwitterionic lipids by hydrogen peroxide: potential implications for apoptosis. *Chem. Sci. 6*, 705−713.
(49) Godoy, L. C., Munoz-Pinedo, C., Castro, L., Cardaci, S., Schonhoff, C. M., King, M., Tortora, V., Marin, M., Miao, Q., Jiang, J. F., Kapralov, A., Jemmerson, R., Silkstone, G. G., Patel, J. N., Evans, J. E., Wilson, M. T., Green, D. R., Kagan, V. E., Radi, R., and Mannick, J. B. (2009) Disruption of the M80-Fe ligation stimulates the translocation of cytochrome c to the cytoplasm and nucleus in nonapoptotic cells. *Proc. Natl. Acad. Sci. U. S. A. 106*, 2653−2658.
(50) Rumbley, J. N., Hoang, L., and Englander, S. W. (2002) Recombinant Equine Cytochrome c in Escherichia coli: High-Level Expression, Characterization, and Folding and Assembly MutantsΓÇá. *Biochemistry 41*, 13894−13901.
(51) Dopner, S., Hildebrandt, P., Grant Mauk, A., Lenk, H., and Stempfle, W. (1996) Analysis of vibrational spectra of multicomponent systems. Application to pH-dependent resonance Raman spectra of ferricytochrome c. *Spectrochim. Acta, Part A 52*, 573−584.
(52) Radi, R., Turrens, J. F., and Freeman, B. A. (1991) Cytochrome c-catalyzed membrane lipid peroxidation by hydrogen peroxide. *Arch. Biochem. Biophys. 288*, 118−125.
(53) Dragomir, I., Hagarman, A., Wallace, C., and Schweitzer-Stenner, R. (2007) Optical band splitting and electronic perturbations of the heme chromophore in cytochrome c at room temperature probed by visible electronic circular dichroism spectroscopy. *Biophys. J. 92*, 989−998.
(54) Battistuzzi, G., Bortolotti, C. A., Bellei, M., Di Rocco, G., Salewski, J., Hildebrandt, P., and Sola, M. (2012) Role of Met80 and Tyr67 in the low-pH conformational equilibria of cytochrome c. *Biochemistry 51*, 5967−5978.
(55) Dopner, S., Hildebrandt, P., Rosell, F. I., and Mauk, A. G. (1998) Alkaline conformational transitions of ferricytochrome c studied by resonance Raman spectroscopy. *J. Am. Chem. Soc. 120*, 11246−11255.
(56) Weinkam, P., Zimmermann, J., Sagle, L. B., Matsuda, S., Dawson, P. E., Wolynes, P. G., and Romesberg, F. E. (2008) Characterization of Alkaline Transitions in Ferricytochrome c Using Carbon−Deuterium Infrared Probes. *Biochemistry 47*, 13470−13480.
(57) Hu, S., Morris, I. K., Singh, J. P., Smith, K. M., and Spiro, T. G. (1993) Complete assignment of cytochrome c resonance Raman spectra via enzymatic reconstitution with isotopically labeled hemes. *J. Am. Chem. Soc. 115*, 12446−12458.
(58) Indiani, C., De Sanctis, G., Neri, F., Santos, H., Smulevich, G., and Coletta, M. (2000) Effect of pH on axial ligand coordination of cytochrome c" from Methylophilus methylotrophus and horse heart cytochrome c. *Biochemistry 39*, 8234−8242.

DOI: 10.1021/acs.biochem.5b00922
Biochemistry 2015, 54, 7491−7504

(59) Othman, S., Le Lirzin, A., and Desbois, A. (1994) Resonance Raman investigation of imidazole and imidazolate complexes of microperoxidase: Characterization of the bis(histidine) axial ligation in c- type cytochromes. *Biochemistry 33*, 15437−15448.
(60) Hammack, B., Godbole, S., and Bowler, B. E. (1998) Cytochrome c folding traps are not due solely to histidine-heme ligation: direct demonstration of a role for N-terminal amino group-heme ligation1. *J. Mol. Biol. 275*, 719−724.
(61) Sanghera, N., and Pinheiro, T. J. T. (2000) Unfolding and refolding of cytochrome c driven by the interaction with lipid micelles. *Protein Sci. 9*, 1194−1202.
(62) Pinheiro, T. J. T., Elove, G. A., Watts, A., and Roder, H. (1997) Structural and Kinetic Description of Cytochrome c Unfolding Induced by the Interaction with Lipid Vesicles. *Biochemistry 36*, 13122−13132.
(63) Chattopadhyay, K., and Mazumdar, S. (2003) Stabilization of partially folded states of cytochrome c in aqueous surfactant: Effects of ionic and hydrophobic interactions. *Biochemistry 42*, 14606−14613.
(64) Rahaman, H., Alam Khan, Md. K., Hassan, M., Islam, A., Moosavi-Movahedi, A. A., and Ahmad, F. (2015) Heterogeneity of equilibrium molten globule state of cytochrome c induced by weak salt denaturants under physiological condition. *PLoS One 10*, e0120465.
(65) Amacher, J. F., Zhong, F., Lisi, G. P., Zhu, M. Q., Alden, S. L., Hoke, K. R., Madden, D. R., and Pletneva, E. V. (2015) A Compact Structure of Cytochrome c Trapped in a Lysine-Ligated State: Loop Refolding and Functional Implications of a Conformational Switch. *J. Am. Chem. Soc. 137*, 8435−8449.
(66) Sinibaldi, F., Droghetti, E., Polticelli, F., Piro, M. C., Di Pierro, D., Ferri, T., Smulevich, G., and Santucci, R. (2011) The effects of ATP and sodium chloride on the cytochrome c-cardiolipin interaction: The contrasting behavior of the horse heart and yeast proteins. *J. Inorg. Biochem. 105*, 1365−1372.
(67) Bergstrom, C. L., Beales, P. A., Lv, Y., Vanderlick, T. K., and Groves, J. T. (2013) Cytochrome c causes pore formation in cardiolipin-containing membranes. *Proc. Natl. Acad. Sci. U. S. A. 110*, 6269−6274.
(68) Quaroni, L., and Smith, W. E. (1999) The nitro stretch as a probe of the environment of nitrophenols and nitrotyrosines. *J. Raman Spectrosc. 30*, 537−542.
(69) Tezcan, F. A., Winkler, J. R., and Gray, H. B. (1998) Effects of Ligation and Folding on Reduction Potentials of Heme Proteins. *J. Am. Chem. Soc. 120*, 13383−13388.
(70) Belikova, N. A., Vladimirov, Y. A., Osipov, A. N., Kapralov, A. A., Tyurin, V. A., Potapovich, M. V., Basova, L. V., Peterson, J., Kurnikov, I. V., and Kagan, V. E. (2006) Peroxidase activity and structural transitions of cytochrome c bound to cardiolipin-containing membranes. *Biochemistry 45*, 4998−5009.
(71) Abe, M., Niibayashi, R., Koubori, S., Moriyama, I., and Miyoshi, H. (2011) Molecular mechanisms for the induction of peroxidase activity of the cytochrome c-cardiolipin complex. *Biochemistry 50*, 8383−8391.
(72) Pecina, P., Borisenko, G. G., Belikova, N. A., Tyurina, Y. Y., Pecinova, A., Lee, I., Samhan-Arias, A. K., Przyklenk, K., Kagan, V. E., and Huttemann, M. (2010) Phosphomimetic Substitution of Cytochrome c Tyrosine 48 Decreases Respiration and Binding to Cardiolipin and Abolishes Ability to Trigger Downstream Caspase Activation. *Biochemistry 49*, 6705−6714.
(73) Ly, H. K., Utesch, T., Diaz-Moreno, I., Garcia-Heredia, J. M., De la Rosa, M. A., and Hildebrandt, P. (2012) Perturbation of the Redox Site Structure of Cytochrome c Variants upon Tyrosine Nitration. *J. Phys. Chem. B 116*, 5694−5702.

DOI: 10.1021/acs.biochem.5b00922
Biochemistry 2015, 54, 7491−7504